

Research Article

Preparation of Prolonged-Circulating Galangin-Loaded Liposomes and Evaluation of Antitumor Efficacy In Vitro and Pharmacokinetics In Vivo

Hui Yao,¹ Hao Lu,¹ Jun Zhang,¹ Xuemei Xue,² Chao Yin,¹ Jun Hu,¹ Rong Zou,¹ Lun Wang,¹ and Hanlin Xu¹ 

¹School of Pharmaceutical, Hubei University of Chinese Medicine, No. 1, Huangjiahu Road, Wuhan 430065, China

²School of Pharmaceutical, Hubei University of Medicine, No. 30, Renmin Road, Shiyan 442000, China

Correspondence should be addressed to Hanlin Xu; xhl@hbtcm.edu.cn

Received 25 September 2018; Accepted 28 November 2018; Published 7 February 2019

Academic Editor: Stefano Bellucci

Copyright © 2019 Hui Yao et al. This is an open access article distributed under the Creative Commons Attribution License, which permits unrestricted use, distribution, and reproduction in any medium, provided the original work is properly cited.

Galangin has been reported to have many pharmacological effects including being anti-inflammatory, antibacterial, and antifungal and a suppressor of vitiligo, Alzheimer's disease, and cancer. The purpose of this research was to characterize and determine the efficacy of the antitumor activity and pharmacokinetics of galangin-loaded PEGylated liposomes compared with free galangin. Galangin-loaded liposomes and galangin-loaded PEGylated liposomes were prepared using thin-film dispersion prior to ultrasonication. The mean particle size of the galangin-loaded PEGylated liposomes was approximately 120 nm, the polydispersity index was 0.212, the zeta potential was -2.24 mV, and the entrapment efficiency was 76.31%. The release of galangin from galangin-loaded PEG-modified liposomes was slowest as gauged by dynamic dialysis *in vitro*. In the apoptosis experiment, galangin-loaded PEG-modified liposomes demonstrated cytotoxicity to hepatoma cells by apoptosis that was greater than the two other forms of drug carrier. *In vivo* experiments demonstrated that the half-life of galangin in PEG-modified liposomes was 4 hours in the plasma of rats, significantly longer than that of free galangin. The experimental results suggest that the PEG modification of liposomes effectively increases the solubility of galangin and alters its pharmacokinetic parameters, such that it may be effective in the treatment of liver cancer.

1. Introduction

Galangin (Gal) is an active flavonoid extracted and isolated from the roots of *Alpinia officinarum* Hance, an annual plant, and has a long history of use as a medicine and edible herb in China to warm the stomach, prevent vomiting, and remove cold and pain. It is also listed in the Chinese Pharmacopoeia [1]. Many studies have reported that galangin possesses a broad range of pharmacological activity such as being anti-inflammatory, antibacterial, and antifungal and suppressing vitiligo, Alzheimer's disease, and cancer [2].

Recent studies have found that galangin can induce apoptosis and promote autophagy [3]. However, it does not easily dissolve in aqueous solution which could limit its potential for clinical use.

In the past decades, researchers have developed many nanotechnological solutions to solubilize poorly soluble drugs. Compared with other nanoformulations, liposomes have many advantages, such as excellent biocompatibility, the capability to enhance absorption of drugs, and the capability to reduce their toxicity; thus, liposomes are a good potential drug delivery system which can improve the solubility of liposoluble drugs [4].

However, a major problem exists with intravenously administered liposomes as they suffer rapid clearance from the blood, possibly due to the adsorption of plasma proteins on their phospholipid membranes allowing more rapid recognition by mononuclear macrophages which phagocytose and clear them from plasma [5]. Therefore, in this study, measures that improve the stability of common liposomes

for intravenous delivery were proposed, including the modification of the liposomal surface with polyethylene glycol to avoid macrophage phagocytosis [6].

Research on galangin has, until now, largely focused on pharmacological activity, with no studies on pharmacokinetics having been reported. We hypothesize that polyethylene glycol (PEG) modification of liposomes could prolong the half-life of circulating liposomes and improve the aqueous solubility and pharmacokinetic properties of galangin loaded within. In this study, we prepared galangin-loaded PEG-modified liposomes and evaluated their targeting to liver cancer cells *in vitro* and the pharmacokinetic parameters *in vivo* in rats.

2. Materials and Methods

2.1. Materials. Galangin was provided by Tauto Biotech (Shanghai, China) with a purity of 98% as measured by high-performance liquid chromatography (HPLC). Soybean phosphatidylcholine (SPC) was purchased from YuanQi Biotech (Wuhan, China), cholesterol (Chol) from Solarbio Science and Technology Co. Ltd. (Beijing, China), methoxy polyethylene glycol phospholipid (MPEG-DSPE) from Yarebio (Shanghai China), phosphate-buffered saline (PBS) from HyClone (Logan, USA), trichloromethane and methyl alcohol from Thermo Fisher Scientific Inc. (Waltham, MA), Sephadex G-50 from Sinopharm Chemical (Shanghai, China), fluorescein isothiocyanate (FITC) and HPLC-grade methyl alcohol from Sigma-Aldrich (St. Louis, USA), and Cell Counting Kit-8 (CCK-8) from Dojindo Laboratories (Kumamoto, Japan). Hep G2 hepatoma cells were supplied by the Shanghai Institute of Biochemistry and Cell Biology. Water was purified using an ultrapure water system (Ulu-pure, Chongqing, China). Where unspecified above, reagents and solvents were of analytical grade.

2.2. Preparation and Characterization of Liposomes Containing Gal. Gal-loaded PEG-modified liposomes and Gal-loaded unmodified liposomes were synthesized using thin-film dispersion. SPC, DSPE-PEG, Chol, and Gal were dissolved in a mixture of trichloromethane/methanol (1:3, *v/v*) in a round flask. The organic solvent was removed using a rotary evaporator (RE-3000, Ya-rong, China) in a 37°C water bath (RE-3000, Ya-rong, China) under vacuum. The high vacuum was maintained for 18 hours after formation of a film in order to remove residual organic solvent. PBS (10 mM, pH 7.0) was added and maintained at 45°C for 50 minutes to obtain a crude dispersion. Probe ultrasound was used to reduce the diameter of particles within the suspension and obtain a semitransparent fine dispersion which was extruded through a polycarbonate filter (to 200 nm) and stored at 4°C prior to use. Gal-loaded liposomes were obtained using the same procedure except that the liposomes were not reacted with DSPE-PEG. For blank liposomes, both Gal and DSPE-PEG were not included.

2.3. Particle Size and Zeta Potential Measurement. The mean diameter, polydispersity index (PDI), and zeta potential of the liposomes were measured by dynamic light scattering

using a Malvern Nano ZS90 (Malvern, UK). Raw data were collected at 25°C at an angle of 90°, each measurement being performed in triplicate.

2.4. Transmission Electron Microscopy. The surface morphology of the liposomes was observed using a transmission electron microscope (TEM, JEM-1400, JEOL, Japan) with a field-emission gun operating at 200 kV. Each liposome sample was placed onto a film-coated copper grid and stained with a 2% solution of phosphotungstic acid for 1 minute at room temperature prior to air drying and inserting into the microscope. Excessive quantities of the sample were removed with filter paper, if necessary.

2.5. Determination of Gal Concentration. The concentration of Gal in each preparation was quantified using an LC1260 HPLC system (Agilent, USA), with a C18 column (4.6 mm × 200 mm, 5 μm, Welch Materials, USA) after elution through a C18 precolumn (4.6 mm × 20 mm; Agilent, USA) at a column temperature of 40°C. The eluate was analyzed at a wavelength of 267 nm. The mobile phase was an aqueous mixture of acetonitrile/phosphoric acid (60 mM/L at a ratio of 65:35, *v/v*) at a flow rate of 0.8 mL/minute. Samples were diluted with methanol and taken 20 μL of the solution for test.

2.6. Entrapment Efficiency. The efficiency of encapsulation of Gal in the liposome preparations was determined using a minicolumn centrifugation technique. Briefly, 100 μL blank liposomes were added to a Sephadex G-50 gel-filled column (5.0 cm × 1.0 cm) to saturation so as to ensure fine recovery. Subsequently, precisely 0.2 mL Gal-loaded PEG-modified liposomes or Gal-loaded unmodified liposomes were added to the top of gel bed followed by 0.2 mL PBS (10 mM, pH 7.0). Care was taken to ensure that the samples did not drain down the side of the column bed. A suitable blend centrifuge was used to spin the column at 1000*g* for 5 minutes to separate free Gal from the liposomes. Column eluate was dissolved in 2 mL methanol and analyzed for Gal. In addition, 0.2 mL Gal-loaded PEG-modified liposomes or Gal-loaded unmodified liposomes mixed with 0.2 mL PBS (10 mM, pH 7.0) and 2 mL methanol were also analyzed for Gal. Entrapment efficiency (EE%) was quantified using the following equation: $EE\% = W_g/W_t \times 100\%$ where W_g = mass of Gal in liposome eluate and W_t = total mass of Gal in liposome dispersion. The concentration of Gal was determined using HPLC as described above.

2.7. In Vitro Release Study. The *in vitro* release of Gal from the liposomes was measured using dynamic dialysis [7] with medium containing 0.4% (*w/v*) sodium lauryl sulfate maintained at 37 ± 0.5°C. Two mL aliquots of Gal-loaded PEG-modified liposome and Gal-loaded unmodified liposome dispersions were pipetted into dialysis bags (MWCO 14,000, Boston, USA). Free Gal was dispersed in an aqueous solution containing 0.2% (*v/v*) Tween-80 to obtain a concentration of 1 mg/mL, then 2 mL was added to the dialysis bags which were then sealed. The dialysis bags were placed into flasks containing 50 mL release medium and stirred at a rotational speed of 100 rpm. A 0.2 mL aliquot of release sample

was withdrawn after 0.5, 1, 2, 3, 4, 5, 6, and 8 hours, which was then centrifuged at 9000g for 10 minutes at 25°C. The concentration of released Gal in the supernatant was measured using HPLC as described above.

2.8. Storage Stability Study. The prepared liposomes were stored at 4°C and mean particle size, polydispersity index, zeta potential, and encapsulation efficiency were measured after 0, 5, 10, 15, and 20 days using the methods described above to assess their stability profile. The leakage ratio was calculated using the formula: leakage ratio = $(W_0 - W_t)/W_0 \times 100\%$ where W_0 = entrapment efficiency on day 0; W_t = entrapment efficiency on day t .

2.9. In Vitro Cytotoxicity Assay. A conventional MTT assay was utilized for analysis of the cytotoxic effects of the formulations against Hep G2 cells. The cells were seeded in 96-well plates at a density of 5.0×10^3 cells/mL [8]. Various dilutions of the three formulations were added to wells and incubated for 24 hours at 37°C in an atmosphere containing 5% CO₂. After the addition of 20 μL MTT to each well, the plates were incubated for a further 4 hours whereupon the culture medium from each well was carefully replaced with 150 μL DMSO to dissolve the formazan crystals. For each well, the absorbance at 570 nm was measured using a microplate reader (Bio-Rad, USA). The metabolic suppression (R%) was calculated using the formula as follows:

$$R\% = \left(\frac{1 - OD_{\text{test}}}{OD_{\text{control}}} \right). \quad (1)$$

Half-maximal inhibitory concentration (IC₅₀) values were computed using SPSS v19.0. Raw data are presented as means and standard deviations ($n = 3$).

2.10. Analysis of Apoptosis. An annexin V-FITC apoptosis kit was used to measure the apoptosis of Hep G2 cells.

2.11. Study of Uptake in Cells. To visualize the endocytosis of the formulations in Hep G2 cells, fluorescein isothiocyanate (FITC), which fluoresces green, was encapsulated in the liposomes as a test drug at a ratio of FITC to liposome of 1:20 (w/w) [9]. Hep G2 cells were seeded in 6-well plates at a density of 1.0×10^5 cells/well and cultured at 37°C in an atmosphere containing 5% CO₂ for 24 hours. Culture medium was replaced by test sample solutions: FITC free, FITC/Gal-loaded unmodified liposomes, and FITC/Gal-loaded PEG-modified liposomes at a FITC dose of 5 μM. The cells were cultured for a further 2 hours and then washed three times with ice-cold PBS to terminate the uptake in cells. Finally, cell fluorescence was imaged using EVOS FL (Thermo Fisher, USA), an autocell imaging system.

2.12. In Vivo Pharmacokinetic Analysis. The pharmacokinetics of Gal-loaded PEG-modified liposomes were compared with those of Gal-loaded liposomes and Gal free in rats after intravenous injections at doses of 5 mg/kg. Male Wistar rats weighing $200 \text{ g} \pm 20 \text{ g}$ were supplied by the laboratory animal center of Hubei University of Chinese Medicine and housed at 25°C ± 1°C at a humidity of 55% ± 5%. All animals were free

to drink and eat *ad libitum* and maintained in a regular 12-hour light/dark cycle. Rats were fasted overnight before dosing and were assigned randomly into 3 groups ($n = 6$ for each time point). The experiment was conducted in accordance with the guidelines of the ethical committee of Hubei University of Chinese Medicine. The liposome formulations were administered directly via the tail vein. After 0.5, 1.0, 2.0, 4.0, 6.0, 8.0, 12.0, and 24.0 hours, 200 μL aliquots of blood were collected from the fossa orbitalis vein into a heparinized tube and then immediately centrifuged at 3000g rpm for 10 minutes. The plasma supernatant of each was removed and stored at -20°C until analyzed.

The concentration of Gal in mouse whole blood was quantified using a modification of the HPLC protocol described above, by adjusting the volume ratio of acetonitrile/phosphoric acid aqueous solution (60 mM) to 55:45 (v/v) as follows. Gal was separated using a previously published liquid-liquid extraction procedure with minor modification [10]. Five hundred μL acetonitrile was added to the separated plasma, vortex mixed for 5 minutes, then centrifuged at 5000g for 15 minutes at 4°C. The organic layer was then transferred to a separate tube and the solvent evaporated using a light stream of nitrogen at 35°C. The residue was redissolved in 50 μL methanol and injected into the HPLC column.

The following pharmacokinetic parameters for each sample were determined from the temporal changes in Gal concentration using DAS 2.1.1 software (issued by the State Food and Drug Administration of China for pharmacokinetic studies): maximum concentration (C_{max}), biological half-life ($T_{1/2}$), area under curve (AUC_{0-t}), and total body clearance (CL).

2.13. Statistical Analysis. Results are presented as means ± SD ($n = 3$). Statistical significance was tested by one-way analysis of variance (ANOVA), using SPSS v19.0 software with data considered statistically significant at $P < 0.05$.

3. Results and Discussion

3.1. Preparation and Characterization of Liposomes Containing Galangin. The results demonstrated that Gal-loaded PEG-modified liposomes can be successfully prepared using thin-film dispersion/ultrasound and that the two liposome preparations presented in this study have suitable particle size and encapsulation efficiencies.

In brief, SPC, Chol, GAL, and DSPE-PEG were simultaneously dissolved in a mixture of trichloromethane/methanol. The initial appearance of the liposomes changed from initial turbidity to a semitransparent state following ultrasonic treatment. This phenomenon suggests that, after sonication, the particle size of the drug decreased to the nanometer scale. Residual organic solvents in the liposomes can be toxic when injected intravenously. In order to remove them, the prepared films were placed under vacuum for more than 12 hours. Meanwhile, PBS (10 mM, pH 7.0) was used as a hydration medium in this experiment.

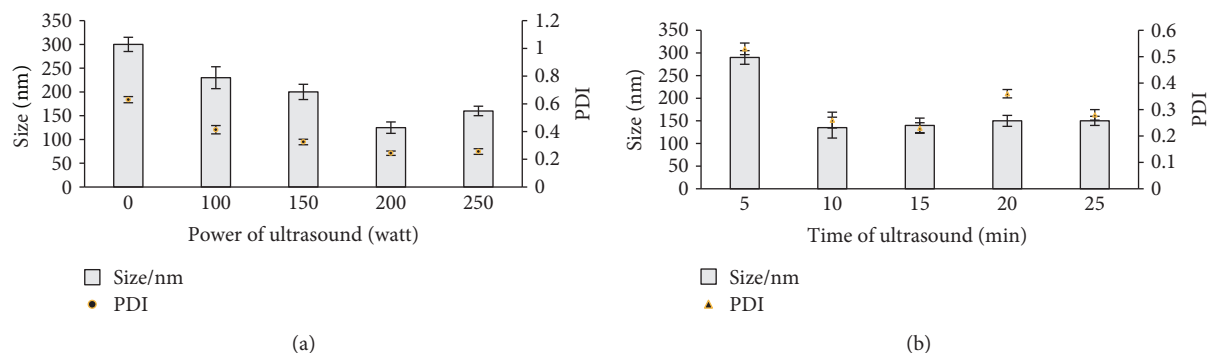


FIGURE 1: (a) The effects of ultrasonic power on the particle size and PDI of Gal-loaded liposomes. Data are presented as mean \pm SD ($n = 3$). (b) The effects of ultrasonic time on the particle size and PDI of Gal-loaded liposomes. Data are presented as mean \pm SD ($n = 3$).

3.2. Observation of Particle Size and Zeta Potential. Studies have demonstrated that the size of liposomes has a great impact on their efficacy both *in vitro* and *in vivo* [11]. For nanoformulations, prolonged circulation and enhanced permeability can be demonstrated when the average particle diameter is greater than the renal filtration cutoff size [12]. Particles smaller than 50 nm can interact with hepatocytes, while particles larger than 1 μm are absorbed by mononuclear phagocytes as emboli [13]. Thus, the influence of various factors on particle size and distribution was initially investigated. The PDI of a preparation indicates the degree of dispersion within it, that is, the similarity of the particle diameters. The smaller the PDI, the more similar are the particles. Generally speaking, a nanodosing preparation for injection should have a PDI value of less than 0.3 [14]. Particle size and PDI were dramatically reduced after probe ultrasound, and the smallest liposome diameters (approximately 125 nm) were achieved with ultrasound power set to 200 W (Figure 1(a)). Since Gal is lipophilic in nature, combination with phospholipid layers results in maintaining it in a more stable state. So a substantial reduction in particle size presented no concerns about the stability of Gal. Both TEM images and the results of the encapsulation assay confirmed the integrity of the structure of the liposomes. When ultrasound power was increased to 250 W, particle size and PDI also increased. Excessive ultrasonic power may destroy the stable vesicles and initiate their aggregation.

In addition, particle size did not change significantly when ultrasound was applied for more than 10 minutes at a power of 200 W (Figure 1(b)). Thus, a power of 200 W and exposure for 10 minutes were chosen to prepare the liposomes for experimental investigation. Furthermore, liposomes prepared by film dispersion often have a multilayered structure [15]. We did not require very small particles because their interfacial tension is too large, and they are prone to aggregation and are unstable [16].

The ratio of SPC/Chol also had a substantial impact on particle size and distribution. It has been reported that Chol can regulate the fluidity of the phospholipid bilayer membrane, reduce membrane permeability, and reduce drug leakage [17]. Particle size reduced substantially as Chol concentration in the bilayer decreased, achieving a particle diameter of approximately 120 nm at an SPC:SDC ratio of

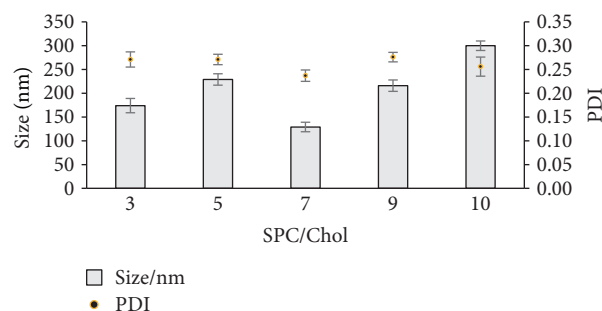


FIGURE 2: Effect of the ratio of SPC/Chol on the particle size and PDI of Gal-loaded liposomes. Data are presented as mean \pm SD ($n = 3$).

7:1. Additional reduction in the proportion of cholesterol lead to an increase in liposome particle size down to an SPC:Chol ratio of 10:1 where the particle size was at its maximum value in this experiment (Figure 2). Similarly, PDI was at its minimum value for an SPC:Chol ratio of 7:1. The cholesterol within the liposome phospholipid bilayer can regulate surface tension and increase elasticity, which may also reduce particle size and PDI [18]. The mean diameter of the final liposome preparations was approximately 125 ± 6 nm, with a narrow PDI (Figure 3(a)). Liposomes with a particle size of less than 200 nm can benefit from the enhanced permeability and retention (EPR) effect observed in tumors [19].

The mean zeta potential of the liposomes was -0.322 ± 0.018 mV (Figure 3(b)). Liposomes carry a small negative charge, which hinders aggregation and fusion and increases stability [20]. PEG-modified liposomes have a more negative zeta potential, possibly due to the presence of a negatively charged phosphate group, as previously reported [21].

The entrapment efficacy of Gal-loaded PEG-modified liposomes and Gal-loaded unmodified liposomes was $79.07 \pm 3.11\%$ and $84.65 \pm 5.98\%$, respectively. The difference may be due to the long-chain portion of PEG covering the liposomes and hindering Gal from entering the internal lipophilic core.

3.3. Morphological Observations by Transmission Electron Microscopy. Figure 4 displays a TEM image of PEG-

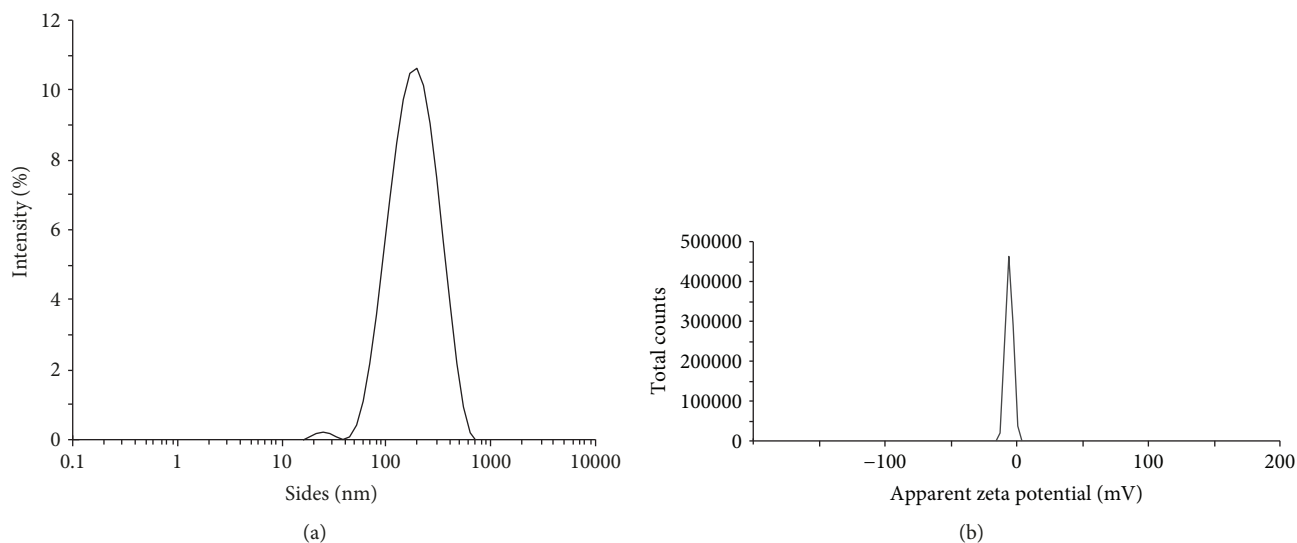


FIGURE 3: (a) The typical particle size and distribution of PEG-modified Gal-loaded liposomes measured by dynamic light scattering. (b) The typical surface zeta potential of PEG-modified Gal-loaded liposomes.

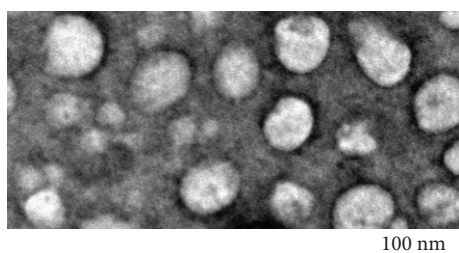


FIGURE 4: Transmission electron microscope images of PEG-modified Gal-loaded liposomes (magnitude 20000x, scale 100 nm).

modified Gal-loaded liposomes. The spherical vesicular structure could easily be observed with a particle size of approximately 120 nm, smaller than that measured by the Nano ZS90. The reason for this discrepancy may be due to differences in sample preparation for the two techniques. The Nano ZS90 measures drug particle size in an aqueous state while TEM requires dry samples. During preparation for TEM, the particles within the sample probably shrank as the medium evaporated.

3.4. In Vitro Release Study. The release profiles of the three Gal formulations are summarized in Figure 5. *In vitro* release of drugs can provide a reference for pharmacokinetic studies *in vivo*.

Gal can be dissolved in aqueous medium and meets the sink condition. The results demonstrate that free Gal diffused into the release medium more quickly than in the other two preparations, with Gal-loaded PEG-modified liposomes releasing the slowest. Eight-hour cumulative release of Gal from the two liposome formulations measured $65.7 \pm 6.4\%$ (PEG modified) and $70.9 \pm 3.5\%$ (unmodified), respectively. The comparative value for Gal solution was $93.3\% \pm 5.3\%$

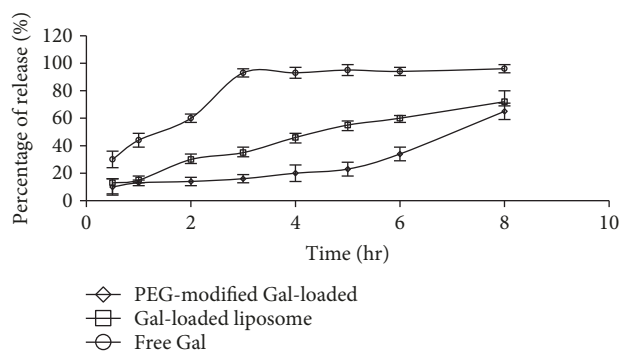


FIGURE 5: *In vitro* release of Gal from PEG-modified liposome, Gal-loaded liposome, and free entity. Data are presented as mean \pm SD ($n = 3$).

within 3 hours. As can be seen, Gal release from the liposomes was relatively rapid within the first 2 hours before subsequently decelerating. The initial rapid release phenomenon may be explained by Gal that was adsorbed on the surface of the liposomes.

The cause of the slow release of Gal from the liposomes may possibly be that liposomes with a PEG-modified surface can change the properties of their hydrated boundary layer and so the permeability of the membrane.

3.5. Storage Stability Study. To examine the stability of the liposomes, a two-week stability study was conducted to ensure their quality when stored at 4°C . Particle size, polydispersity index, entrapment efficiency, and zeta potential were measured at a set time point after preparation. The stability profiles of Gal-loaded PEG-modified liposomes and Gal-loaded unmodified liposomes are shown in Tables 1 and 2. For PEG-modified liposomes, the observed parameters changed slightly compared to the Gal-loaded liposomes

TABLE 1: The stability of PEG-modified Gal-loaded liposomes for 14 days stored in 4°C ($n = 3$).

Time (days)	Size (nm)	PDI	Zeta potential (mV)	Entrapment efficiency (%)	Leakage ratio (%)
0	124.67 ± 1.53	0.23 ± 0.02	-1.39 ± 0.06	83.33 ± 1.53	0 ± 0
3	125.67 ± 4.51	0.24 ± 0.02	-1.84 ± 0.44	81.33 ± 1.53	2.40 ± 1.83
6	132.67 ± 4.73	0.23 ± 0.03	-2.05 ± 0.09	80.33 ± 0.58	3.60 ± 0.69
12	157.00 ± 4.58	0.27 ± 0.03	-1.72 ± 0.61	78.33 ± 3.06	6.00 ± 3.67
14	168.00 ± 2.02	0.24 ± 0.02	-2.04 ± 0.16	79.01 ± 1.11	5.23 ± 1.23

TABLE 2: The stability of Gal-loaded liposomes for 14 days stored in 4°C ($n = 3$).

Time (days)	Size (nm)	PDI	Zeta potential (mV)	Entrapment efficiency (%)	Leakage ratio (%)
0	114.33 ± 5.13	0.21 ± 0.01	-1.79 ± 0.41	84.67 ± 1.53	0 ± 0
3	132.67 ± 9.45	0.25 ± 0.02	-1.93 ± 0.09	84.23 ± 2.52	1.57 ± 2.97
6	190.67 ± 2.08	0.31 ± 0.02	-2.01 ± 0.6	76.12 ± 2.01	10.24 ± 2.36
12	204.67 ± 10.12	0.34 ± 0.02	-1.81 ± 0.68	71.33 ± 1.53	15.75 ± 1.8
14	231.33 ± 15.57	0.34 ± 0.02	-1.83 ± 0.7	70.67 ± 1.15	16.54 ± 1.36

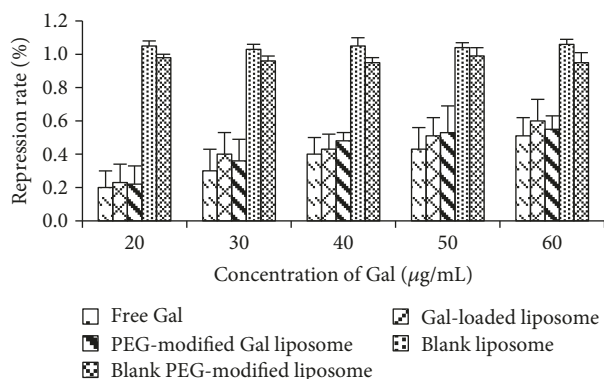


FIGURE 6: In vitro cytotoxicity of PEG-modified Gal-loaded liposomes, Gal-loaded liposomes, free Gal, blank liposomes, and blank PEGylated liposomes against HepG2 cells.

which could be attributed to PEGylation reducing the agglomeration rate of the liposomes by covering their surface and causing steric hindrance [22]. We can deduce that the prepared Gal-loaded PEG-modified liposomes are relatively stable.

3.6. In Vitro Cytotoxicity Assay. To assess the anticancer potential of Gal, we studied the cytotoxicity of free Gal, Gal-loaded liposomes, and Gal-loaded PEG-modified liposomes against Hep G2 cells *in vitro* using an MTT assay. As shown in Figure 6, the metabolic suppression of Hep G2 cells differed in free Gal, Gal-loaded liposomes, and Gal-loaded PEG-modified liposomes after 24 hours of culture. At the same concentration level, the PEG-modified liposome group demonstrated a strong inhibition of Hep G2 cells compared to the other two groups. The calculated half-maximal inhibitory concentration (IC₅₀) values of Gal, Gal-loaded

liposomes, and Gal-loaded PEG-modified liposomes were 65 µg/mL, 55 mg/mL, and 43 µg/mL, respectively. These results indicate that the introduction of a prolonged circulating delivery system could be beneficial in exerting a strong cytotoxicity against Hep G2 cells, which demonstrated that PEG-mediated endocytosis can promote cellular uptake and thus enhance the cytotoxic effect of PEG-modified liposomes [23].

3.7. Analysis of Apoptosis. Annexin V-FITC and PI were used to investigate the ability of the different preparations to induce apoptosis or necrosis in Hep G2 cells. As shown in Figure 7(a), the total proportion of apoptotic cells due to Gal loading of unmodified and PEG-modified liposomes was 18.5% and 22.9%, respectively. For a concentration of Gal of 50 µg/mL in PEG-modified liposomes, a 1.34-fold rise in total apoptosis of Hep G2 cells compared with Gal-loaded unmodified liposomes was observed. A statistical analysis is displayed in Figure 7(b). One can speculate that after incubation with Hep G2 cells, free Gal is released from Gal-loaded PEG-modified liposomes and induce apoptosis in Hep G2 cells.

3.8. In Vivo Pharmacodynamics Study. To examine the prolongation of release of Gal from liposomes, Gal-loaded PEG-modified liposomes were compared with Gal-loaded unmodified liposomes and free Gal in rats. Plasma concentrations of galangin from the three formulations are shown in Figure 8, and the pharmacokinetic parameters calculated by DAS 2.1.1 software are shown in Table 3. The results demonstrate that for the majority of parameters, significant differences exist from the different forms. The $T_{1/2}$ of Gal-loaded PEG-modified liposomes was approximately 2.7 times longer than that of free Gal ($P < 0.01$) and 1.7 times longer than that of Gal-loaded unmodified liposomes ($P < 0.05$). Although the C_{max} of Gal-loaded PEG-modified

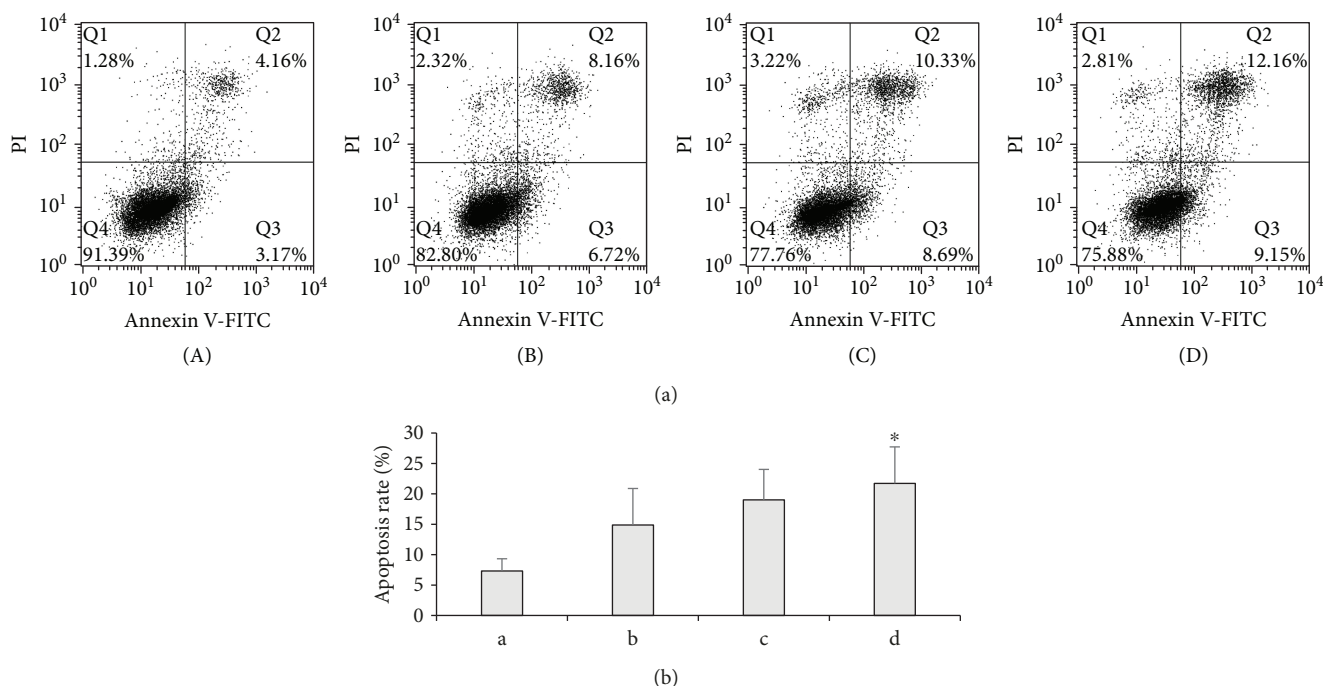


FIGURE 7: (a) Flow cytometric analysis of cell apoptosis in Hep G2 cells after staining with annexin V-FITC and PI: (A) control, (B) free Gal, (C) Gal-loaded liposome, and (D) PEG-modified Gal-loaded liposome. (b) Apoptosis rate are shown as histograms. Data are presented as mean \pm SD ($n = 3$), * $P < 0.05$ versus free Gal liposome.

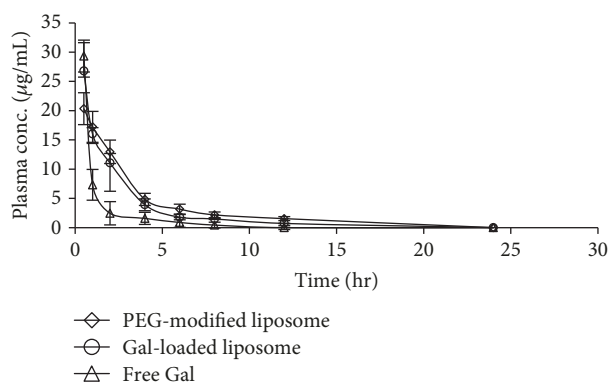


FIGURE 8: The plasma concentration of Gal versus time after a single intravenous injection dose of 5 mg/kg equivalent PEG-modified Gal-loaded liposomes, Gal-loaded liposomes, and free Gal in rats. Data are presented as mean \pm SD ($n = 6$).

liposomes was the smallest of all preparations, the $AUC_{(0-t)}$ ratios of PEG-modified liposomes to free Gal and to Gal-loaded unmodified liposomes were approximately 1.5-fold ($P < 0.05$) and 1.1-fold ($P < 0.05$), respectively. However, the V_d and CL values for both Gal-loaded liposome formulations were significantly lower than those for free Gal.

These data suggest that free Gal was rapidly cleared in the blood circulation. Liposome preparations increased its concentration in plasma and withstood its clearance after intravenous administration. Furthermore, modification with

PEG enhanced this effect. The possible reason for this difference is that liposomes, after modification with PEG, can be protected and avoid macrophage phagocytosis, thus prolonging the concentration of the drug in plasma [24].

However, the mechanisms of this process require further elucidation *in vivo*.

Galangin is a flavonol compound with a high content in galangal and has a variety of pharmacological activities. The researchers found that galangin can effectively inhibit the invasion and migration of HepG2 cells induced by TPA. This inhibition is achieved by the protein kinase C/extracellular signal-regulated kinase pathway [25]. Quercetin is also a flavonol compound that has been extensively studied and proven to have multiple biological activities. Some scholars have investigated the biological activity of galangin and quercetin on human gastric cancer cells (SGC-7910). It is found that galangin can inhibit cell growth, induce apoptosis, and decrease mitochondrial membrane potential more effectively than quercetin [26]. From this point of view, we believe that galangin has a good potential medicinal value, and it is worthy of further in-depth formulation research.

4. Conclusions

The present study demonstrated that PEG-modified liposomes containing Gal could be prepared using thin-film dispersion followed by ultrasonic probe treatment. The entrapment efficiency of Gal was 80% with little leakage of Gal under experimental storage conditions. Compared with free Gal, the solubility, antitumor efficacy, and

TABLE 3: Pharmacokinetic parameters after intravenous injection of PEG-modified Gal-loaded liposomes, Gal-loaded liposomes, and free Gal ($n = 6$).

Parameters	Free Gal	Gal-loaded liposomes	PEG-modified liposomes
t1/2 (h)	1.531 ± 0.171	2.461 ± 0.546	4.088 ± 1.171
Cmax (µg/mL)	33.223 ± 1.961	26.798 ± 4.951	21.282 ± 1.961
AUC0–6 h (mg/L·h)	49.939 ± 8.576	67.398 ± 8.733	74.203 ± 8.576
AUC0–∞ h (mg/L·h)	51.122 ± 11.901	69.042 ± 8.507	81.909 ± 11.901
MRT 0–t (h)	1.338 ± 0.164	2.331 ± 0.187	3.011 ± 0.164
MRT 0–∞ (h)	1.563 ± 0.446	2.793 ± 0.289	4.666 ± 0.446

pharmacokinetics of PEG-modified liposomes were improved. These results suggest that Gal-loaded PEG-modified liposomes appear to be a possible drug delivery system for cancer.

Data Availability

The data used to support the findings of this study are available from the corresponding author upon request.

Conflicts of Interest

The authors declare no conflict of interest.

Authors' Contributions

Hui Yao and Hao Lu contributed equally to this work.

Acknowledgments

This work was supported by Qing Miao project of Hubei University of Chinese Medicine.

References

- [1] Q. Liu, W. Luyten, K. Pellens et al., "Antifungal activity in plants from Chinese traditional and folk medicine," *Journal of Ethnopharmacology*, vol. 143, no. 3, pp. 772–778, 2012.
- [2] L. P. Zhu, Q. Q. Luo, J. J. Bi, J. Y. Ding, S. F. Ge, and F. X. Chen, "Galangin inhibits growth of human head and neck squamous carcinoma cells *in vitro* and *in vivo*," *Chemico-Biological Interactions*, vol. 224, pp. 149–156, 2014.
- [3] X. Li, Y. J. Wang, Y. Z. Xiong et al., "Galangin induces autophagy via deacetylation of LC3 by SIRT1 in HepG2 cells," *Scientific Reports*, vol. 6, no. 1, article 30496, 2016.
- [4] E. Agostinelli, F. Vianello, G. Magliulo, T. Thomas, and T. J. Thomas, "Nanoparticle strategies for cancer therapeutics: nucleic acids, polyamines, bovine serum amine oxidase and iron oxide nanoparticles (review)," *International Journal of Oncology*, vol. 46, no. 1, pp. 5–16, 2015.
- [5] F. Yu and X. H. Tang, "Novel long-circulating liposomes consisting of PEG modified β -sitosterol for gambogic acid delivery," *Journal of Nanoscience and Nanotechnology*, vol. 16, no. 3, pp. 3115–3121, 2016.
- [6] K. Abe, K. Higashi, K. Watabe et al., "Effects of the PEG molecular weight of a PEG-lipid and cholesterol on PEG chain flexibility on liposome surfaces," *Colloids and Surfaces A: Physicochemical and Engineering Aspects*, vol. 474, pp. 63–70, 2015.
- [7] L. Q. Wang, "Preparation and *in vitro* evaluation of an acidic environment-responsive liposome for paclitaxel tumor targeting," *Asian Journal of Pharmaceutical Sciences*, vol. 12, no. 5, pp. 470–477, 2017.
- [8] M. Nasr, N. Nafee, H. Saad, and A. Kazem, "Improved antitumor activity and reduced cardiotoxicity of epirubicin using hepatocyte-targeted nanoparticles combined with tocotrienols against hepatocellular carcinoma in mice," *European Journal of Pharmaceutics and Biopharmaceutics*, vol. 88, no. 1, pp. 216–225, 2014.
- [9] M. J. Liu, D. Qu, Y. Chen, C. Y. Liu, Y. P. Liu, and X. F. Ding, "Preparation of novel butyryl galactose ester-modified coix component microemulsions and evaluation on hepatoma-targeting *in vitro* and *in vivo*," *Drug Delivery*, vol. 23, no. 9, pp. 3444–3451, 2016.
- [10] Z. K. Han, Z. N. Liu, L. Yuan, P. S. Zhang, and M. Zhao, "Preparation of paraoxonase-1 liposomes and studies on their *in vivo* pharmacokinetics in rats," *Clinical and Experimental Pharmacology and Physiology*, vol. 41, no. 10, pp. 825–829, 2014.
- [11] W. Sun, W. Zou, G. Huang, A. Li, and N. Zhang, "Pharmacokinetics and targeting property of TFu-loaded liposomes with different sizes after intravenous and oral administration," *Journal of Drug Targeting*, vol. 16, no. 5, pp. 357–365, 2008.
- [12] H. Soo Choi, W. Liu, P. Misra et al., "Renal clearance of quantum dots," *Nature Biotechnology*, vol. 25, no. 10, pp. 1165–1170, 2007.
- [13] C. Contado, E. Vighi, A. Dalpiaz, and E. Leo, "Influence of secondary preparative parameters and aging effects on PLGA particle size distribution: a sedimentation field flow fractionation investigation," *Analytical and Bioanalytical Chemistry*, vol. 405, no. 2-3, pp. 703–711, 2013.
- [14] K. Higashisaka, K. Nagano, Y. Yoshioka, and Y. Tsutsumi, "Nano-safety research: examining the associations among the biological effects of nanoparticles and their physicochemical properties and kinetics," *Biological & Pharmaceutical Bulletin*, vol. 40, no. 3, pp. 243–248, 2017.
- [15] Y. P. Patil and S. Jadhav, "Novel methods for liposome preparation," *Chemistry and Physics of Lipids*, vol. 177, pp. 8–18, 2014.
- [16] S. Deshpande, Y. Caspi, A. E. C. Meijering, and C. Dekker, "Octanol-assisted liposome assembly on chip," *Nature Communications*, vol. 7, no. 1, 2016.
- [17] S. Kaddah, N. Khreich, F. Kaddah, C. Charcosset, and H. Greige-Gerges, "Cholesterol modulates the liposome membrane fluidity and permeability for a hydrophilic molecule," *Food and Chemical Toxicology*, vol. 113, pp. 40–48, 2018.

- [18] H. Furuhashi, K. Tomita, T. Teratani et al., "Vitamin A-coupled liposome system targeting free cholesterol accumulation in hepatic stellate cells offers a beneficial therapeutic strategy for liver fibrosis," *Hepatology Research*, vol. 48, no. 5, pp. 397–407, 2018.
- [19] H. Gao, S. Zhang, S. Cao, Z. Yang, Z. Pang, and X. Jiang, "Angiopep-2 and activatable cell-penetrating peptide dual-functionalized nanoparticles for systemic glioma-targeting delivery," *Molecular Pharmaceutics*, vol. 11, no. 8, pp. 2755–2763, 2014.
- [20] M. A. De Luca, F. Lai, F. Corrias et al., "Lactoferrin- and antitransferrin-modified liposomes for brain targeting of the NK3 receptor agonist senktide: preparation and in vivo evaluation," *International Journal of Pharmaceutics*, vol. 479, no. 1, pp. 129–137, 2015.
- [21] Y. Cheng, M. Liu, H. J. Hu, D. Z. Liu, and S. Y. Zhou, "Development, optimization, and characterization of PEGylated nanoemulsion of prostaglandin E1 for long circulation," *AAPS PharmSciTech*, vol. 17, no. 2, pp. 409–417, 2016.
- [22] D. Pozzi, V. Colapicchioni, G. Caracciolo et al., "Effect of polyethyleneglycol (PEG) chain length on the bio-nano-interactions between PEGylated lipid nanoparticles and biological fluids: from nanostructure to uptake in cancer cells," *Nanoscale*, vol. 6, no. 5, pp. 2782–2792, 2014.
- [23] Y. Li, D. D. Yang, Y. Zhang, and C. Y. Zhu, "Novel DSPE-PEG-cholic acid-modified liposomes with hepatic targeting properties improve the anti-tumor efficacy of oral doxorubicin hydrochloride for liver tumor-bearing mice," *Journal of Biomedical Nanotechnology*, vol. 13, no. 6, pp. 727–736, 2017.
- [24] W. Yang, S. J. Liu, T. Bai et al., "Poly (carboxybetaine) nanomaterials enable long circulation and prevent polymer-specific antibody production," *Nano Today*, vol. 9, no. 1, pp. 10–16, 2014.
- [25] S. T. Chien, M. D. Shi, Y. C. Lee, C. C. Te, and Y. W. Shih, "Galangin, a novel dietary flavonoid, attenuates metastatic feature via PKC/ERK signaling pathway in TPA-treated liver cancer HepG2 cells," *Cancer Cell International*, vol. 15, no. 1, p. 15, 2015.
- [26] Y. X. Xu, B. Wang, and X. H. Zhao, "In vitro effects and the related molecular mechanism of galangin and quercetin on human gastric cancer cell line (SGC-7901)," *Pakistan Journal of Pharmaceutical Sciences*, vol. 30, no. 4, pp. 1279–1287, 2017.

